

Influence of Density Functionals and Basis Sets on One-Bond Carbon–Carbon NMR Spin–Spin Coupling Constants

R. Suardíaz,[†] C. Pérez,[†] R. Crespo-Otero,[†] José M. García de la Vega,^{*,‡} and Jesús San Fabián[‡]

Departamento de Química Física, Facultad de Química, Universidad de la Habana, La Habana 10400, Cuba, and Departamento de Química Física Aplicada, Facultad de Ciencias, Universidad Autónoma de Madrid, 28049 Madrid, Spain

Received December 4, 2007

Abstract: The basis set and the functional dependence of one-bond carbon–carbon NMR spin–spin coupling constants (SSCC) have been analyzed using density functional theory. Four basis sets (6-311G**, TZVP, EPR-III, and aug-cc-pVTZ-J) and four functionals (PBE, PW91, B3LYP, and B3P86) are tested by comparison with 70 experimental values corresponding to 49 molecules that represent multiple types of hybridization of the carbon atoms. The two hybrid functionals B3P86 and B3LYP combined either EPR-III or aug-cc-pVTZ-J basis sets lead to the best accuracy of calculated SSCC. However, a simple linear regression allows for the obtaining of scaled coupling constants that fit much better with the experimental data and where the differences between the different basis sets and/or functional results are significantly reduced. For large molecules the TZVP basis set can be an appropriate election presenting a good compromise between quality of results and computational cost.

1. Introduction

Spin–spin coupling constants (SSCC) represent a valuable source of structural information from nuclear magnetic resonance (NMR) spectroscopy. During the past decade, the use of quantum chemistry methods for the calculation of SSCC has become routine and widespread.^{1–3} Predictions from wavefunction-based methods are generally in good agreement with experimental values.^{4–6} Nevertheless, the high computational cost required by these methods limits their applicability to small systems. Density functional theory (DFT) methodology combined with analytical linear response techniques is a promising alternative to post Hartree–Fock methods. However, the bibliographic DFT data related to the calculation of SSCC show certain dispersion in the functional and basis sets employed.^{6–12} There are various works reporting that B3LYP^{13,14} functional yields satisfactory results for SSCC in a small set of molecules.^{7–9} On the other

hand, Maximoff et al.⁶ reported the assessment of 20 different functionals in predicting one-bond carbon–hydrogen. In this work,⁶ the best results were reported for PBE^{15,16} and PW91^{17–19} functionals, both based on the gradient generalized approximation (GGA), and report a good performance⁶ for the semiempirical-hybrid B3P86,^{13,20} whereas B3LYP resulted in one of the worst. They conclude that meta-GGA and hybrid functionals do not necessarily improve over GGA functionals for this type of couplings. Keal et al.¹¹ tested functionals B97-2²¹ and B97-3²² with the data set of Maximoff et al.⁶ The performance of PBE, B97-2, B97-3, and B3LYP for predicting other kinds of couplings that include N, O, and F elements in 11 alternative molecules were also carried out by Keal et al.¹¹ They reported that PBE was considerably less accurate than B3LYP for the prediction of those SSCC. Recently, Witanowski et al.¹² studied 257 aromatic carbon–carbon couplings across one, two, and three bonds. They obtained excellent calculated values using the B3PW91/6-311++G(d,p)//B3PW91/6-311++G(d,p) approach where the same functional-basis set combination was employed for geometry optimizations and for coupling

* Corresponding author e-mail: garcia.delavega@uam.es.

[†] Universidad de la Habana.

[‡] Universidad Autónoma de Madrid.

constants computation. Other functionals have been tested with a variety of results.²³

With regards to basis sets, it is well-known that calculated SSCC strongly depend on the quality of the employed Gaussian basis set functions. The Fermi contact (FC) term usually provides the largest contribution. Therefore, the electronic density at the nucleus should be well described, and, consequently, the selection of the basis set is crucial in SSCC calculations. Several basis sets can be found in the literature² to calculate coupling constants. The work of Peralta et al.²⁴ constitutes, to our knowledge, one of the largest analyses within the DFT framework. These authors analyzed basis set dependence using the B3LYP functional. In that work, some well-known basis set functions were employed, namely IGLO-III,²⁵ EPR-III,^{26,27} aug-cc-pVTZ-J,²⁸ and Sadlej-J.²⁹ The authors suggested the combination B3LYP/aug-cc-pVTZ-J as an excellent choice to calculate SSCC.

One-bond carbon–carbon is the most important bond in organic chemistry, and carbon–carbon coupling constants $^1J_{CC}$ possess unique structural information concerning electronic structure, substituent effects, and stereochemical behavior of organic molecules.³⁰ The hybridization state of the two carbons offers a variety of six different types of bonds and a large range for $^1J_{CC}$. The aim of the present work is to investigate the capabilities of a different combination of functionals and basis sets to predict, with a certain degree of accuracy, the one-bond carbon–carbon coupling constants ($^1J_{CC}$) of organic molecules containing elements of the first and second rows of the periodic table. This goal will be performed using a statistical analysis by comparing the calculated $^1J_{CC}$ with the experimental ones.

2. Computational Details

We have selected four exchange-correlation functionals among the large number available in the literature. The two first GGA functionals were PBE^{15,16} and PW91.^{17–19} Those functionals had the best performance among 20 other tested by Maximoff et al.⁶ for the calculation of $^1J_{CH}$. The two second hybrid functionals were B3P86^{13,20} and B3LYP.^{13,14} The former functional yielded similar performance to those of PBE and PW91 for $^1J_{CH}$, while the latter has been used successfully by some authors,^{7,24} although it has been reported as one of the worst by Maximoff et al.⁶

Computations were performed using four basis sets of contracted Gaussian functions, namely 6-311G**,^{31,32} TZVP,³³ EPR-III,^{26,27} and aug-cc-pVTZ-J.²⁸ 6-311G** is a small basis set with a triple- ζ quality plus polarization. TZVP is a DFT-optimized valence triple- ζ basis with promising results in the prediction of hyperfine couplings in combination with the B3LYP functional.³⁴ EPR-III is larger and has been optimized for the computation of hyperfine coupling constants by DFT methods with the s-part improved to better describe the nuclear region. EPR-III is a triple- ζ basis including diffuse functions, doubled-polarizations, and a single set of f-polarization functions. aug-cc-pVTZ-J is a relatively large basis set, specially designed for the computation of SSCC. aug-cc-pVTZ-J is a recontraction of aug-cc-pVTZ-Juc,²⁸ that is the triple- ζ aug-cc-pVTZ^{35–39} of Dunning

completely uncontracted, augmented with four tight s-type functions and without the most diffuse second polarization function. The computational cost of the calculations depends on the complexity of the approximate functional expressions and the basis set dimensions. Thus, computational time estimated by Maximoff et al.⁶ in C₆H₅NO₂ (514 basis functions) is for the hybrid functionals B3LYP and B3P86 five times larger than for the GGA functionals PBE and PW91. For the molecules calculated in this work, the average computational time for the B3LYP and B3P86 functionals is roughly twice that of the PBE and PW91 ones, when the EPR-III and aug-cc-pVTZ-J basis sets are used. However, the computational time for all functionals is similar when 6-311G** and TZVP are used. Moreover, larger differences are found for the approximated average computational cost of the different basis sets: TZVP is twice as expensive as 6-311G**; EPR-III is between 5 (with PBE or PW91 functionals) and 9 (with B3LYP or B3P86 functionals) times more expensive; and the large basis set aug-cc-pVTZ-J is between 15 (with PBE or PW91 functionals) and 34 (with B3LYP or B3P86 functionals) times more expensive. The computational time for these two large basis set is very dependent on the used functional.

In this study we have considered a set of organic molecules containing first and second row elements. The basic criteria for the selection of the systems have been the rigidity or, at least, the existence of only one populated conformer. We determined $^1J_{CC}$ for these 49 chemically diverse molecules that correspond to 70 experimentally measured one-bond carbon–carbon couplings involving 19 $^1J_{C_{sp^3}-C_{sp^3}}$, 11 $^1J_{C_{sp^3}-C_{sp^2}}$, 6 $^1J_{C_{sp^3}-C_{sp}}$, 29 $^1J_{C_{sp^2}-C_{sp^2}}$, 2 $^1J_{C_{sp^2}-C_{sp}}$, and 3 $^1J_{C_{sp}-C_{sp}}$. This set was mainly extracted from the reports of Wray and Krivdin et al.^{30,40–49} (see the Supporting Information for specific references). Since accurate experimental geometries are only available for a few molecules in this set, we used optimized geometries at the B3LYP/6-31G** level of theory, which is considered sufficiently accurate for the present purpose.^{34,50} The set of selected molecules are depicted in Figure 1. Although rovibrational effects can be non-negligible in SSCC^{51,52} we do not consider them in this report since their evaluation is computational demanding.⁵³ Evaluation of solvent effect in small molecules has shown a reduced sensitivity. This effect is mainly due to reaction field effects via the indirect contribution from equilibrium geometry changes.^{52,54} The geometrical parameters that more significantly affect the SSCC are the dihedral angles but in selected molecules were essentially constant due to their rigidity. Hence solvent effects are also neglected. All computations were performed using the Gaussian03 package.⁵⁵

3. Results and Discussion

The 70 coupling constants calculated with four functionals and four basis sets have been analyzed by means of statistical methods. An initial exploration makes us withdraw 6 coupling constants from the data set used in the statistics due to their large deviation. For this reason, these 6 calculated values are analyzed at the end of this section. The statistical analysis has been carried out over three sets of couplings: i) **Set-1** formed by the whole set of couplings (64 values);

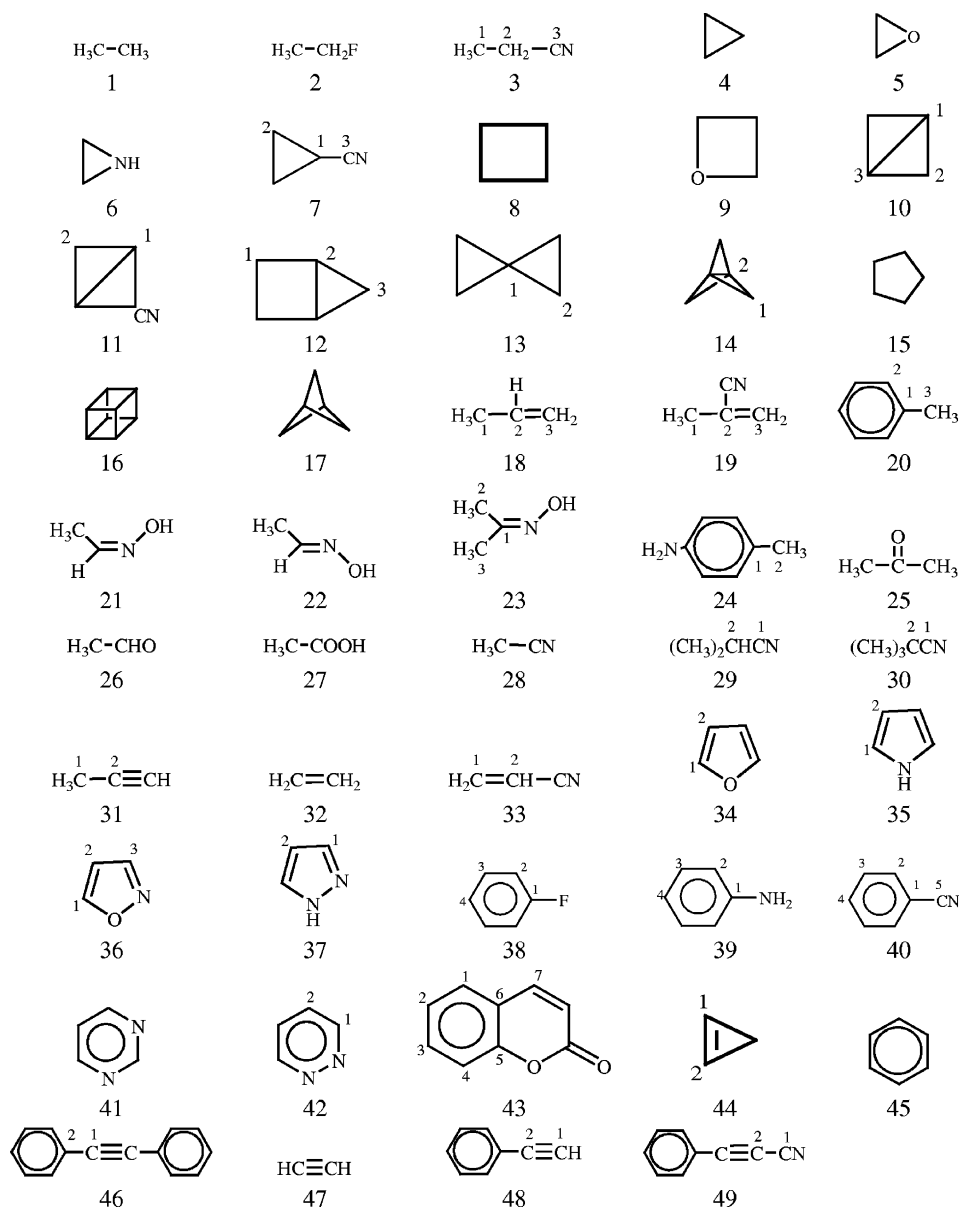


Figure 1. Studied molecules.

ii) **Set-2** with couplings smaller than 46 Hz (26 values), i.e. it includes 18 $C_{sp^3}-C_{sp^3}$ and the 8 smaller $C_{sp^3}-C_{sp^2}$ values; and iii) **Set-3** with couplings larger than 46 Hz (38 values) which include 6 $C_{sp^3}-C_{sp}$, 27 $C_{sp^2}-C_{sp^2}$, 2 $C_{sp^2}-C_{sp}$, and the 3 larger $C_{sp^3}-C_{sp^2}$ values. The election of these data sets of couplings is based on the graphical behavior in which there seems to be a change of the tendency around 46 Hz (see Figure 2).

The statistics for the three data sets presented in Tables 1–3 is based on the values of standard deviation (σ), mean absolute error (MAE), and the minimum (Min) and maximum (Max) deviation

$$\sigma = \sqrt{\frac{\sum (J_{CC}^{exp} - J_{CC}^{calc})^2}{n-1}}, \quad MAE = \frac{\sum |J_{CC}^{exp} - J_{CC}^{calc}|}{n} \quad (1)$$

Most of the calculated couplings underestimate the experimental values. Therefore, the calculated values can be shifted and/or scaled to obtain better estimations and to detect whether the differences between the results are either merely

quantitative or qualitative. Scaled couplings were obtained by a simple linear expression

$$J_{CC}^{scaled} = a + b \cdot J_{CC}^{calc} \quad (2)$$

The coefficients a and b were calculated by fitting the calculated couplings for each approach (functional/basis set) to the equation $J_{CC}^{exp} = a + b \cdot J_{CC}^{calc}$. A standard deviation (σ'), mean absolute error (MAE'), and minimum (Min') and maximum (Max') deviation for these fitted values are also considered and included in Tables 1–3.

$$\sigma' = \sqrt{\frac{\sum [J_{CC}^{exp} - (a + b \cdot J_{CC}^{calc})]^2}{n-2}}, \quad MAE' = \frac{\sum |J_{CC}^{exp} - (a + b \cdot J_{CC}^{calc})|}{n} \quad (3)$$

Set-1 includes all calculated couplings (except the six indicated below), and it has an experimental range between 10 and 91 Hz. For this set, the best result is that of the B3P86/

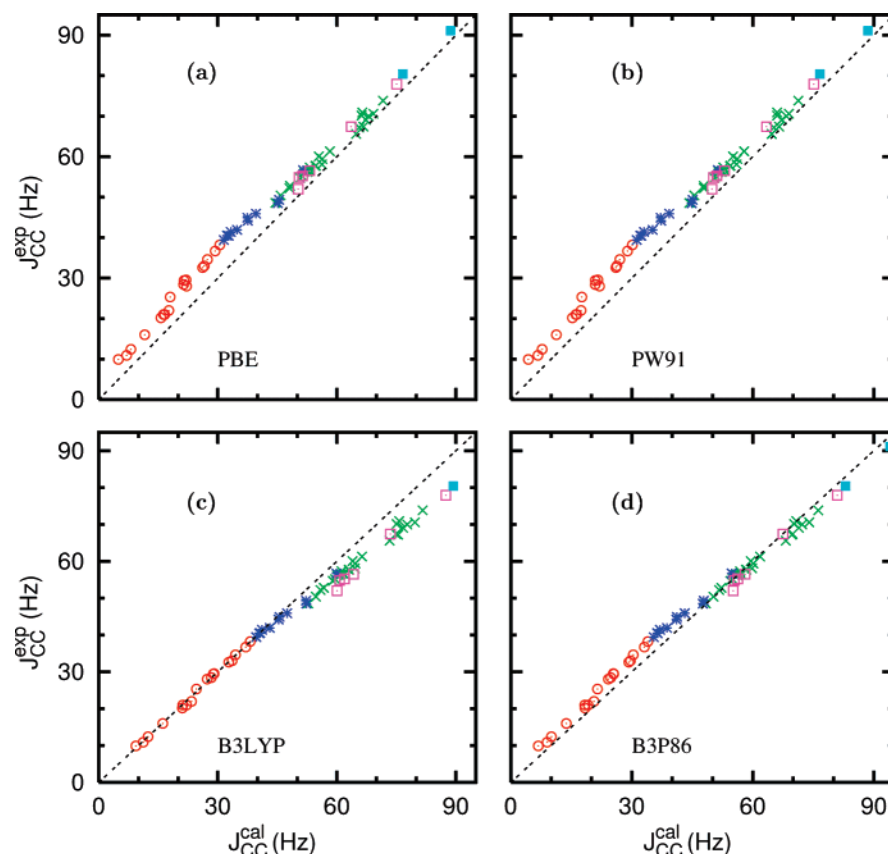


Figure 2. Experimental vs calculated $^1J_{CC}$ couplings. aug-cc-pVTZ-J basis were used for the four indicated functionals: $^1J_{C_{sp^3}-C_{sp^3}}$ (\circ), $^1J_{C_{sp^3}-C_{sp^2}}$ (*), $^1J_{C_{sp^2}-C_{sp^2}}$ (\times), $^1J_{C_{sp^3}-C_{sp}}$ (\square), $^1J_{C_{sp^2}-C_{sp}}$ (\blacksquare).

Table 1. Statistical Results for 64 Data (Set-1) Calculated Using the Indicated Functional/Basis Set (in Hz)

functional/basis set	σ	MAE	Max	Min	a ^a	b ^a	σ'	MAE'	Max'	Min'
PBE/6-311G**	3.53	2.81	4.4	-8.4	7.2(6)	0.87(1)	2.01	1.69	3.9	-4.0
PBE/TZVP	4.58	3.75	1.0	-8.9	8.5(5)	0.89(1)	1.63	1.32	2.9	-3.4
PBE/EPR-III	6.53	6.31	-3.5	-9.3	7.4(4)	0.97(1)	1.43	1.14	2.8	-3.0
PBE/aug-cc-pVTZ-J	4.98	4.54	-0.7	-8.1	7.4(5)	0.93(1)	1.52	1.23	2.9	-3.1
PW91/6-311G**	4.33	3.39	4.1	-10.3	8.4(6)	0.88(1)	2.06	1.71	4.2	-4.2
PW91/TZVP	5.64	4.91	0.1	-10.5	9.5(5)	0.90(1)	1.66	1.33	3.0	-3.6
PW91/EPR-III	6.69	6.46	-3.5	-9.5	7.7(4)	0.97(1)	1.44	1.14	2.8	-3.0
PW91/aug-cc-pVTZ-J	5.25	4.81	-0.9	-8.4	7.8(5)	0.93(1)	1.53	1.23	2.8	-3.1
B3LYP/6-311G**	7.10	5.69	12.9	-2.3	4.3(6)	0.82(1)	1.82	1.48	3.1	-4.1
B3LYP/TZVP	5.98	4.66	12.3	-1.6	4.8(5)	0.83(1)	1.39	1.12	2.4	-3.5
B3LYP/EPR-III	2.92	2.28	6.8	-1.7	3.4(4)	0.90(1)	1.28	1.02	2.2	-3.7
B3LYP/aug-cc-pVTZ-J	4.72	3.63	9.6	-0.7	3.5(4)	0.87(1)	1.30	1.07	2.3	-3.5
B3P86/6-311G**	3.52	3.15	6.0	-6.4	6.6(6)	0.86(1)	1.85	1.54	3.1	-3.7
B3P86/TZVP	3.24	2.64	4.8	-5.9	7.2(5)	0.87(1)	1.45	1.16	2.6	-3.3
B3P86/EPR-III	3.17	2.70	1.3	-5.7	5.4(4)	0.94(1)	1.29	1.04	2.4	-3.5
B3P86/aug-cc-pVTZ-J	2.49	2.03	3.4	-4.4	5.4(4)	0.91(1)	1.34	1.08	2.5	-3.3

^a The error in the last digit is given between parentheses.

aug-cc-pVTZ-J with a σ deviation of 2.5 Hz (MAE = 2.0 Hz). Other results with σ values smaller than 4 Hz are those of B3LYP/EPR-III (σ = 2.9 Hz), B3P86/EPR-III (σ = 3.2 Hz), B3P86/TZVP (σ = 3.2 Hz), B3P86/6-311G** (σ = 3.5 Hz), and the inexpensive PBE/6-311G** (σ = 3.5 Hz).

When the calculated values are fitted to eq 2, the scaled couplings achieve σ' deviations in a narrow interval (between 1.3 and 2.1 Hz). The best results (σ' smaller than 1.35 Hz) are obtained with the B3P86 and B3LYP functionals and with the EPR-III and aug-cc-pVTZ-J basis sets. The positive

intercepts and the slopes that are always smaller than one indicate that the smaller calculated couplings are more underestimated than the larger ones. The intercepts are larger for BPE and PW91 functionals than for B3LYP and B3P86 ones.

For Set-2 (couplings in the range between 10 and 46 Hz) the best results are those obtained with the B3LYP functional that presents σ deviations between 0.7 (when the aug-cc-pVTZ-J basis set is used) and 1.4 Hz (with the 6-311G** basis set). For the coupling constants involving sp^3 carbons

Table 2. Statistical Results for 26 Data (Set-2) Calculated Using the Indicated Functional/Basis Set (in Hz)

functional/basis set	σ	MAE	Max	Min	a ^a	b ^a	σ'	MAE'	Max'	Min'
PBE/6-311G**	5.04	4.65	-1.9	-8.4	2.8(9)	1.07(3)	1.58	1.09	4.1	-2.3
PBE/TZVP	6.76	6.49	-4.4	-8.9	4.9(6)	1.07(2)	1.22	0.99	2.6	-2.1
PBE/EPR-III	7.59	7.26	-4.3	-9.3	4.0(5)	1.14(2)	0.93	0.79	1.6	-1.8
PBE/aug-cc-pVTZ-J	6.65	6.37	-3.9	-8.1	3.8(5)	1.11(2)	0.98	0.82	1.8	-1.7
PW91/6-311G**	6.48	6.08	-3.1	-10.3	4.4(9)	1.07(4)	1.79	1.31	4.6	-2.6
PW91/TZVP	7.91	7.61	-5.3	-10.5	6.2(7)	1.06(3)	1.43	1.20	3.1	-2.2
PW91/EPR-III	7.79	7.47	-4.5	-9.5	4.4(5)	1.13(2)	1.00	0.87	1.8	-1.7
PW91/aug-cc-pVTZ-J	6.96	6.67	-4.2	-8.4	4.3(5)	1.10(2)	1.05	0.91	2.0	-1.6
B3LYP/6-311G**	1.42	1.24	2.4	-2.3	0.2(7)	0.97(2)	1.13	0.80	2.8	-1.9
B3LYP/TZVP	1.03	0.78	2.3	-1.6	1.5(5)	0.95(1)	0.85	0.69	1.5	-1.5
B3LYP/EPR-III	0.98	0.83	0.5	-1.7	0.5(3)	1.01(1)	0.60	0.48	1.0	-1.2
B3LYP/aug-cc-pVTZ-J	0.69	0.52	1.6	-0.7	0.3(4)	0.98(1)	0.63	0.50	0.9	-1.3
B3P86/6-311G**	3.71	3.39	-0.8	-6.4	2.5(7)	1.03(3)	1.33	0.96	3.2	-2.3
B3P86/TZVP	4.52	4.32	-2.4	-5.9	3.8(5)	1.02(2)	1.02	0.84	1.7	-1.8
B3P86/EPR-III	4.41	4.20	-2.2	-5.7	2.2(4)	1.08(1)	0.72	0.58	0.9	-1.5
B3P86/aug-cc-pVTZ-J	3.44	3.26	-1.4	-4.4	2.0(4)	1.05(1)	0.74	0.60	0.9	-1.6

^a The error in the last digit is given between parentheses.**Table 3.** Statistical Results for 38 Data (Set-3) Calculated Using the Indicated Functional/Basis Set (in Hz)

functional/basis set	σ	MAE	Max	Min	a ^a	b ^a	σ'	MAE'	Max'	Min'
PBE/6-311G**	2.02	1.56	4.4	-2.5	4.5(1)	0.91(2)	1.33	1.02	3.0	-2.4
PBE/TZVP	2.21	1.87	1.0	-4.2	7.3(1)	0.91(1)	0.96	0.71	2.0	-2.0
PBE/EPR-III	5.82	5.66	-3.5	-7.4	6.9(1)	0.98(2)	0.95	0.71	1.9	-2.3
PBE/aug-cc-pVTZ-J	3.51	3.29	-0.7	-5.2	6.5(1)	0.94(2)	0.98	0.75	1.7	-2.1
PW91/6-311G**	1.88	1.55	4.1	-4.3	6.6(1)	0.90(2)	1.44	1.07	2.9	-3.4
PW91/TZVP	3.43	3.07	0.1	-5.6	8.9(1)	0.90(2)	1.02	0.76	2.2	-2.1
PW91/EPR-III	5.93	5.77	-3.5	-7.5	7.5(1)	0.97(2)	0.96	0.71	2.0	-2.3
PW91/aug-cc-pVTZ-J	3.77	3.54	-0.9	-5.4	7.2(1)	0.94(2)	1.00	0.76	1.9	-2.2
B3LYP/6-311G**	9.19	8.74	12.9	3.8	2.9(2)	0.83(2)	1.56	1.14	3.0	-3.6
B3LYP/TZVP	7.76	7.31	12.3	3.8	4.6(1)	0.83(2)	1.14	0.81	2.5	-3.3
B3LYP/EPR-III	3.72	3.28	6.8	1.2	3.8(1)	0.89(2)	1.20	0.87	2.3	-3.6
B3LYP/aug-cc-pVTZ-J	6.13	5.76	9.6	2.9	3.3(1)	0.86(2)	1.14	0.85	2.2	-3.2
B3P86/6-311G**	3.43	2.98	6.0	-1.5	5.2(1)	0.88(2)	1.37	1.02	3.2	-3.2
B3P86/TZVP	2.01	1.49	4.8	-2.2	7.1(1)	0.87(1)	0.97	0.67	2.2	-3.0
B3P86/EPR-III	2.00	1.68	1.3	-3.8	5.7(1)	0.93(2)	0.99	0.71	1.9	-3.3
B3P86/aug-cc-pVTZ-J	1.61	1.19	3.4	-1.9	5.3(1)	0.90(2)	0.98	0.73	2.0	-3.0

^a The error in the last digit is given between parentheses.

the B3LYP functional gives the best results. It should be noted the very good results obtained with the inexpensive TZVP basis set. The values calculated with the B3P86 functional present a deviation between 3.4 and 4.5 Hz, and those obtained with PBE and PW91 show higher deviations (between 5.0 and 7.9 Hz). For $^1J_{C_{sp3}-C_{sp3}}$ couplings, the PBE, PW91, and B3P86 functionals give values smaller than the experimental ones. Using the values scaled with eq 2 the σ' deviations are also smaller for B3LYP results, but for the three other functionals the reduction of the standard deviations is very significant. The σ' values for PW91, PBE, B3P86, and B3LYP with the EPR-III basis set are 1.0, 0.9, 0.7, and 0.6 Hz, respectively.

For Set-3 (couplings in the range between 48 and 91 Hz) the best results are those of B3P86/aug-cc-pVTZ-J ($\sigma = 1.6$ Hz), PW91/6-311G** (1.9 Hz), B3P86/EPR-III (2.0 Hz), B3P86/TZVP (2.0 Hz), PBE/6-311G** (2.0 Hz), and PBE/TZVP (2.2 Hz). The B3P86 seems to yield the best results for this set even with the economic TZVP. On the other hand, the frequently used B3LYP functional presents here larger standard deviations (between 3.8 and 9.2 Hz). Again the use

of scaled values reduces significantly the standard deviations. It is worth mentioning that the best results can be obtained with the PBE, PW91, or B3P86 functionals which present a σ' values around 1.0 Hz when one of the three larger basis sets are used. It is also important regarding the large reduction in the standard deviation for the B3LYP results from σ (between 3.8 and 9.2 Hz) to σ' (between 1.2 and 1.6 Hz).

With regards to the basis sets, for the three sets the worse σ' results are obtained by 6-311G**. The σ values for this basis set are also large for the hybrid functionals results; however, these σ deviations are relatively good when the GGA functionals are used, in part, due to a compensation of errors. For the scaled couplings, the basis sets EPR-III and aug-cc-pVTZ-J provide similar results, whereas TZVP presents slightly worse σ' values, except for set-3 in which results similar to those of the two other basis sets are obtained. Taking into account i) the reasonable σ' results for the TZVP basis set, ii) the low σ values for B3LYP/TZVP in set-2 (1.0 Hz) and for B3P86/TZVP and PBE/TZVP in set-3 (2.0 and 2.2 Hz, respectively), and iii) the compu-

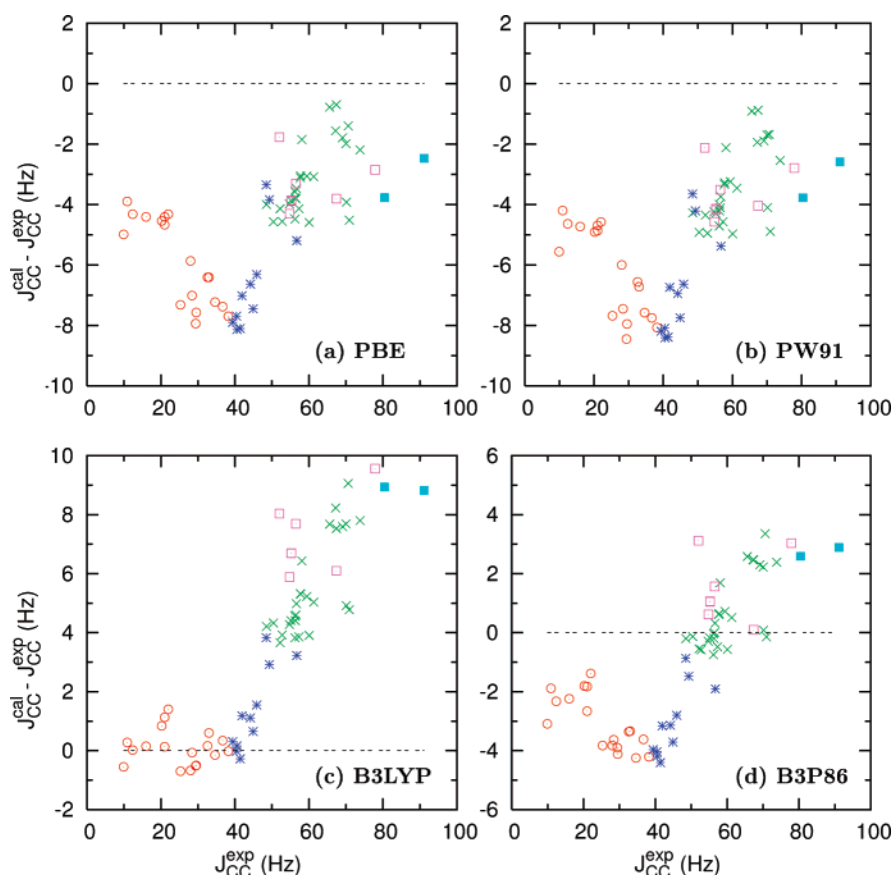


Figure 3. Calculated deviations ($J_{CC}^{cal} - J_{CC}^{exp}$) vs experimental values. aug-cc-pVTZ-J basis were used for the four functionals: $^1J_{C_{sp3}-C_{sp3}}$ (○), $^1J_{C_{sp3}-C_{sp2}}$ (*), $^1J_{C_{sp2}-C_{sp2}}$ (×), $^1J_{C_{sp3}-C_{sp}}$ (□), $^1J_{C_{sp2}-C_{sp}}$ (■).

tational cost of this basis set, we consider that TZVP is an appropriate election for large molecules.

A more detailed analysis of the functional can be performed representing the differences between the calculated and experimental values (Figure 3). The range of deviations is similar for all functionals, between 0 and −9 Hz for PBE and PW91 results, between −5 and 4 Hz for B3P86, and between −1 and 10 Hz (the largest one) for B3LYP. The calculated PBE and PW91 couplings are always smaller than the experimental, and, as it has already been found for $^1J_{CH}$ coupling,⁶ both functionals give similar results. This fact is due to PBE is essentially a simplification of the PW91 where several fundamental constants are imposed on the energy functional.¹⁵ The B3LYP results for couplings smaller than 46 Hz (Set-2) agree satisfactorily with the experimental data with a deviation between −1 and 2 Hz. However, the deviation for coupling larger than 46 Hz is between 2 and 10 Hz (see Figure 3).

It is also interesting to represent the differences between the results of two functionals or two basis sets to prevent possible distortions from the experimental values (see the Supporting Information). As indicated above, PBE and PW91 functionals give similar results, and the differences between them are smaller than 0.6 Hz in magnitude. Accordingly, the figures of the differences between B3LYP (or B3P86) results and those of PBE are similar to the differences of the former functional with PW91. The differences between PBE (or PW91) and B3LYP are in the range of −4 to −13

Hz, and, roughly, they follow a linear relation with the calculated value, i.e., the deviations are larger for large calculated values. The differences between PBE (or PW91) and B3P86 also follow the linear dependence, but now the range of the deviations, between −1 and −6 Hz, is smaller. A similar linear dependence and range of differences are observed between B3P86 and B3LYP. It should be noted that the relative difference $(J_{CC}^{cal} - J_{CC}^{exp})/J_{CC}^{cal}$ always decreases as the calculated coupling value increases. With regards to the basis sets, in Figure 4 the differences between the results of two basis sets are presented (see also the Supporting Information). The differences between the results of the 6-311G** and any of the three other basis sets are rather scattered. However, the differences between these last basis sets present a linear relation as shown in Figure 4b.

It is interesting to analyze and make some comments about the six above-mentioned experimental couplings that have been removed from the data set used in the statistics. Three of them are the $^1J_{C_{sp}-C_{sp}}$ couplings that present large experimental values (between 155.8 and 175.9 Hz), see Table 4, and introduce a strong distortion in the fits. On the other hand, the number of this type of couplings is too small to get statistical results. However, we tested how they fit with the scaled coupling constants. If these couplings are scaled using eq 2 with the coefficients a and b of Table 1, they present an average deviation defined as $\sum_{methods} (|J_{CC}^{exp} - J_{CC}^{scaled}|)/16$ of −12.6, −8.6, and 3.5 Hz (see Table 4). For

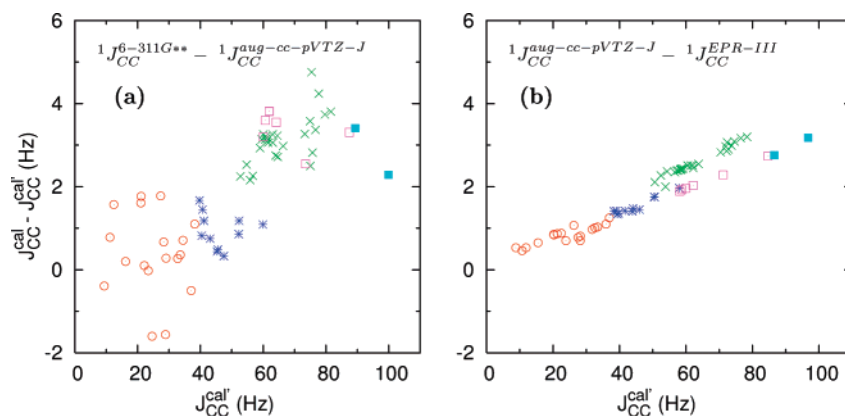
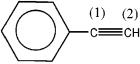
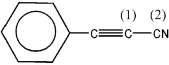
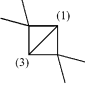
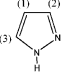
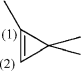


Figure 4. Differences between the results of two different basis sets ($1J_{CC}^{cal} - 1J_{CC}^{cal}$ vs $1J_{CC}^{cal}$). B3LYP functional were used: $1J_{C_{sp3}-C_{sp3}}$ (○), $1J_{C_{sp3}-C_{sp2}}$ (*), $1J_{C_{sp2}-C_{sp2}}$ (×), $1J_{C_{sp3}-C_{sp}}$ (□), $1J_{C_{sp2}-C_{sp}}$ (■).

Table 4. Coupling Constants with the Large Calculated Deviations

No.	Molecule	type	$1J_{CC}^{exp}$ (Hz)	Average deviation ^a (Hz)	
				Initial	Reevaluated
47	HC≡CH	$sp-sp$	170.6	-12.6	—
48		$sp-sp$	175.9	-8.6	—
49		$sp-sp$	155.8	3.5	—
50		sp^3-sp^3	-17.49	-9.2 ^b	-5.7
37		sp^2-sp^2	58.29	6.5 ^c	-0.9
51		sp^2-sp^2	59.1	-4.8 ^d	-0.8

^a Defined as $\sum_{methods} \{1J_{CC}^{exp} - 1J_{CC}^{scaled}\} / \{16\}$. ^b Calculated on unsubstituted bicyclo[1.1.0]butane (molecule 10 in Figure 1). ^c Considering the static molecule instead of the dynamic tautomerism. ^d Calculated on the unsubstituted cyclopropene (molecule 44 in Figure 1) and considering an experimental coupling of 57.1 Hz.

acetylene, this large average deviation (−12.6 Hz) can be explained, in part, with the zero-point vibrational (ZPV) correction (−10.0 Hz) recently calculated by Ruden et al.⁵³ It is reasonable to ascribe a similar ZPV correction to phenylacetylene that explains also the large and negative deviation for the calculated couplings of this molecule. The deviation for the phenylethynyl cyanide is small (3.9 Hz), albeit, the coupling $1J_{C_{sp}-C_{sp}}$ is through a single bond. Therefore, it is reasonable to think that the ZPV correction should be different from that of acetylene.

Three additional values were eliminated in the statistics because they show large deviations if comparing with the remaining calculated couplings. For these couplings (see Table 4) the averaged deviations are −9.2, 6.5, and −4.8 Hz. A detailed analysis of these molecules shows that the reported values actually correspond to derivatives. In the case

of bicyclo[1.1.0]butane⁴³ the reported value was derived from that in 2,2,4,4-tetramethylbicyclo[1.1.0]butane.⁵⁶ Using this last molecule to calculate the $1J_{C_1C_3}$ value and scaling them with eq 2 the average deviation reduces to −5.7 Hz. It should be noted that this coupling is the only one that presents a negative value, and this sign is reproduced in all the calculations. The reported value for cyclopropene (57.1 Hz) corresponds to that of 1,3,3-trimethylcyclopropene (59.1 Hz) corrected by 2 Hz for the methyl substitution.⁵⁷ When the coupling for 1,3,3-trimethylcyclopropene is calculated and scaled, the deviation reduces to 0.8 Hz. The last molecule that presents a large deviation is the pyrazole. We initially compared the experimental couplings with the values calculated for $1J_{C_1C_2}$ in the static molecule. However, this molecule presents a dynamic tautomerism, and the experimental coupling is an average between $1J_{C_1C_2}$ and $1J_{C_1C_3}$ (see

Table 4). Considering this average calculated coupling and scaling them using eq 2 the average deviation reduces to -0.9 Hz.

It is interesting to note that the deviations for each of these six couplings are in the same direction, independently of the approach used (see Table 5 in the Supporting Information).

4. Conclusions

A set of 70 $^1J_{CC}$ coupling constants has been calculated with four functionals and four basis sets. From this set, 64 $^1J_{CC}$ couplings have been used for the statistical analysis. Compared with the experimental data, the standard deviations for B3P86/aug-cc-pVTZ-J and B3LYP/EPR-III results are 2.5 and 2.9 Hz, respectively, which are excellent considering the range of experimental values (between 10 and 91 Hz) and that the vibrational averaging effects have not been included.

B3LYP/aug-cc-pVTZ-J gives the best agreement between calculated and experimental SSCC smaller than 46 Hz ($\sigma = 0.7$ Hz), while B3P86/aug-cc-pVTZ-J results are better for all calculated values ($\sigma = 2.5$ Hz) and for SSCC larger than 46 Hz ($\sigma = 1.6$ Hz).

The standard deviations for the couplings scaled using either the equation $^1J_{CC} = 3.4 + 0.90 \cdot ^1J_{CC}^{B3LYP/EPR-III}$ or the equation $^1J_{CC} = 5.4 + 0.94 \cdot ^1J_{CC}^{B3P86/EPR-III}$ reduce to 1.3 Hz. It is interesting to note that the scaling of the economical PBE/EPR-III results achieves a standard deviation of 1.4 Hz, suggesting that the main trends on the coupling constants also are correctly represented by this functional/basis set combination. It should be noted that the good agreement with experimental obtained for the SSCC is larger than 46 Hz (set-2) with the GGA functional, PBE ($\sigma = 0.9$ Hz) and PW91 ($\sigma = 0.9$ Hz).

The TZVP basis set is suitable for large molecules due to the reduced computational cost and the reasonable results for scaled and nonscaled couplings. Couplings $^1J_{CC}$ smaller than 46 Hz can be calculated using the combination B3LYP/TZVP ($\sigma = 1.0$ Hz), while larger couplings can be obtained with B3P86/TZVP ($\sigma = 2.0$ Hz) or PBE/TZVP ($\sigma = 2.2$ Hz). The whole set of couplings can be calculated with this basis set using B3P86 ($\sigma = 3.2$ Hz).

Larger deviations found in 6 $^1J_{CC}$ couplings have been analyzed. These deviations in the scaled couplings suggest discrepancies between both calculated and experimental data, which allow for the correction of possible mistakes in the data set.

Acknowledgment. J.M.G.V. and J.S.F. gratefully acknowledge the financial support from the Dirección General de Enseñanza Superior e Investigación Científica of Spain (DGESIC, projects: CTQ2005-04469, CTQ2007-66547, and CTQ2007-63332). R.S. and R.C.O. acknowledge a research fellowship from Universidad Autónoma de Madrid. Computer time provided by the Centro de Computación Científica of Universidad Autónoma de Madrid is gratefully acknowledged.

Supporting Information Available: All calculated NMR coupling constants. This material is available free of charge via the Internet at <http://pubs.acs.org>.

References

- (1) Cremer, D.; Gräfenstein, J. *Phys. Chem. Chem. Phys.* **2007**, *9*, 2791.
- (2) Krivdin, L. B.; Contreras, R. H. *Annu. Rep. NMR Spectrosc.* **2007**, *61*, 133.
- (3) Vaara, J. *Phys. Chem. Chem. Phys.* **2007**, *9*, 5399.
- (4) Helgaker, T.; Jaszuński, M.; Ruud, K. *Chem. Rev.* **1999**, *99*, 293.
- (5) Fukui, H. *Prog. Nucl. Magn. Reson. Spectrosc.* **1999**, *35*, 267.
- (6) Maximoff, S. N.; Peralta, J. E.; Barone, V.; Scuseria, G. E. *J. Chem. Theory Comput.* **2005**, *1*, 541.
- (7) Sychrovský, V.; Gräfenstein, J.; Cremer, D. *J. Chem. Phys.* **2000**, *113*, 3530.
- (8) Helgaker, T.; Watson, M.; Handy, N. C. *J. Chem. Phys.* **2000**, *113*, 9402.
- (9) Lantto, P.; Vaara, J.; Helgaker, T. *J. Chem. Phys.* **2002**, *117*, 5998.
- (10) Keal, T. W.; Tozer, D. J.; Helgaker, T. *Chem. Phys. Lett.* **2004**, *391*, 374.
- (11) Keal, T. W.; Helgaker, T.; Salek, P.; Tozer, D. J. *Chem. Phys. Lett.* **2006**, *425*, 163.
- (12) Witanowski, M.; Kamieńska-Trela, K.; Biedrzycka, Z. *J. Mol. Struct.* **2007**, *844–845*, 13.
- (13) Becke, A. D. *J. Chem. Phys.* **1993**, *98*, 5648.
- (14) Lee, C.; Yang, W.; Parr, R. G. *Phys. Rev. B* **1988**, *37*, 785.
- (15) Perdew, J. P.; Burke, K.; Ernzerhof, M. *Phys. Rev. Lett.* **1996**, *77*, 3865.
- (16) Perdew, J. P.; Burke, K.; Ernzerhof, M. *Phys. Rev. Lett.* **1997**, *78*, 1396.
- (17) Perdew, J. P. Unified theory of the exchange and correlation beyond the local density approximation. In *Electronic Structure of Solids '91*; Ziesche, P., Eschrig, H., Eds.; Akademie Verlag: Berlin, 1991; pp 11–20.
- (18) Perdew, J. P.; Chevary, J. A.; Vosko, S. H.; Jackson, K. A.; Peterson, M. R.; Singh, D. J.; Fiolhais, C. *Phys. Rev. B* **1992**, *46*, 6671.
- (19) Perdew, J. P.; Chevary, J. A.; Vosko, S. H.; Jackson, K. A.; Peterson, M. R.; Singh, D. J.; Fiolhais, C. *Phys. Rev. B* **1993**, *48*, 4978.
- (20) Perdew, J. P. *Phys. Rev. B* **1986**, *33*, 8822.
- (21) Wilson, P. J.; Bradley, T. J.; Tozer, D. J. *J. Chem. Phys.* **2001**, *115*, 9233.
- (22) Keal, T. W.; Tozer, D. J. *J. Chem. Phys.* **2005**, *123*, 121103.
- (23) Patchkovskii, S.; Autschbach, J.; Ziegler, T. *J. Chem. Phys.* **2001**, *115*, 26.
- (24) Peralta, J. E.; Scuseria, G. E.; Cheeseman, J. R.; Frisch, M. J. *Chem. Phys. Lett.* **2003**, *375*, 452.
- (25) Schindler, M.; Kutzelnigg, W. *J. Chem. Phys.* **1982**, *76*, 1919.
- (26) Barone, V. *J. Chem. Phys.* **1994**, *101*, 6834.
- (27) Barone, V. Structure, Magnetic Properties and Reactivities of Open-Shell Species from Density Functional and Self-Consistent Hybrid Methods. In *Recent Advances in Density Functional Methods Part I*; Chong, D. P., Ed.; World Scientific Publ. Co.: Singapore, 1996; pp 287–334.

- (28) Provasi, P. F.; Aucar, G. A.; Sauer, S. P. A. *J. Chem. Phys.* **2001**, *115*, 1324.
- (29) Sadlej, J. *Collect. Czech. Chem. Commun.* **1988**, *53*, 1995.
- (30) Krivdin, L. B.; Kalabin, G. A. *Prog. NMR Spectrosc.* **1989**, *22*, 293.
- (31) McLean, A. D.; Chandler, G. S. *J. Chem. Phys.* **1980**, *72*, 5639.
- (32) Krishnan, R.; Binkley, J. S.; Seeger, R.; Pople, J. A. *J. Chem. Phys.* **1980**, *72*, 650.
- (33) Godbout, N.; Salahub, D. R.; Andzelm, J.; Wimmer, E. *Can. J. Chem.* **1992**, *70*, 560.
- (34) Hermosilla, L.; Calle, P.; García de la Vega, J. M.; Sieiro, C. *J. Phys. Chem. A* **2005**, *109*, 1114.
- (35) Dunning, T. H., Jr. *J. Chem. Phys.* **1989**, *90*, 1007.
- (36) Peterson, K. A.; Woon, D. E.; Dunning, T. H., Jr. *J. Chem. Phys.* **1994**, *100*, 7410.
- (37) Wilson, A. K.; van Mourik, T.; Dunning, T. H., Jr. *J. Mol. Struct. (Theochem)* **1996**, *388*, 339.
- (38) Wilson, A. K.; Woon, D. E.; Peterson, K. A.; Dunning, T. H., Jr. *J. Chem. Phys.* **1999**, *110*, 7667.
- (39) Woon, D. E.; Dunning, T. H., Jr. *J. Chem. Phys.* **1995**, *103*, 4572.
- (40) Wray, V. *Prog. NMR Spectrosc.* **1979**, *13*, 177.
- (41) Kaski, J.; Lantto, P.; Vaara, J.; Jokisaari, J. *J. Am. Chem. Soc.* **1998**, *120*, 3993.
- (42) Krivdin, L. B.; Sauer, S. P. A.; Peralta, J. E.; Contreras, R. H. *Magn. Reson. Chem.* **2002**, *40*, 187.
- (43) Krivdin, L. B. *Magn. Reson. Chem.* **2003**, *41*, 91.
- (44) Krivdin, L. B. *Magn. Reson. Chem.* **2002**, *41*, 157.
- (45) Krivdin, L. B. *Magn. Reson. Chem.* **2003**, *41*, 417.
- (46) Krivdin, L. B. *Magn. Reson. Chem.* **2004**, *42*, S168.
- (47) Sauer, S. P. A.; Krivdin, L. B. *Magn. Reson. Chem.* **2004**, *42*, 671.
- (48) Ruden, T. A.; Helgaker, T.; Jaszuński, M. *Chem. Phys.* **2004**, *296*, 53.
- (49) Krivdin, L. B. *Magn. Reson. Chem.* **2005**, *43*, 101.
- (50) Suardíaz, R.; Pérez, C.; García de la Vega, J. M.; San Fabián, J.; Contreras, R. H. *Chem. Phys. Lett.* **2007**, *442*, 119.
- (51) Oddershede, J.; Geertsen, J.; Scuseria, G. E. *J. Phys. Chem.* **1988**, *92*, 3056.
- (52) Contreras, R. H.; Peralta, J. E.; Giribet, C. G.; de Azua, M. C. R.; Facelli, J. C. *Annu. Rep. NMR Spectrosc.* **2000**, *41*, 55.
- (53) Ruden, T. A.; Lutnæs, O. B.; Helgaker, T.; Ruud, K. *J. Chem. Phys.* **2003**, *118*, 9572.
- (54) Ruud, K.; Frediani, L.; Cammi, R.; Mennucci, B. *Int. J. Mol. Sci.* **2003**, *4*, 119.
- (55) Frisch, M. J.; Trucks, G. W.; Schlegel, H. B.; Scuseria, G. E.; Robb, M. A.; Cheeseman, J. R.; Montgomery, J. A., Jr.; Vreven, T.; K. N. K.; Burant, J. C.; Millam, J. M.; Iyengar, S. S.; Tomasi, J.; Barone, V.; Mennucci, B.; Cossi, M.; Scalmani, G.; Rega, N.; Petersson, G. A.; Nakatsuji, H.; Hada, M.; Ehara, M.; Toyota, K.; Fukuda, R.; Hasegawa, J.; Ishida, M.; Nakajima, T.; Honda, Y.; Kitao, O.; Nakai, H.; Klene, M.; Li, X.; Knox, J. E.; Hratchian, H. P.; Cross, J. B.; Bakken, V.; Adamo, C.; Jaramillo, J.; Gomperts, R.; Stratmann, R. E.; Yazyev, O.; Austin, A. J.; Cammi, R.; Pomelli, C.; Ochterski, J. W.; Ayala, P. Y.; Morokuma, K.; Voth, G. A.; Salvador, P.; Dannenberg, J. J.; Zakrzewski, V. G.; Dapprich, S.; Daniels, A. D.; Strain, M. C.; Farkas, O.; Malick, D. K.; Rabuck, A. D.; Raghavachari, K.; Foresman, J. B.; Ortiz, J. V.; Cui, Q.; Baboul, A. G.; Clifford, S.; Cioslowski, J.; Stefanov, B. B.; Liu, G.; Liashenko, A.; Piskorz, P.; Komaromi, I.; Martin, R. L.; Fox, D. J.; Keith, T.; Al-Laham, M. A.; Peng, C. Y.; Nanayakkara, A.; Challacombe, M.; Gill, P. M. W.; Johnson, B.; Chen, W.; Wong, M. W.; Gonzalez, C.; Pople, J. A. *Gaussian 03, Revision D.01*; Gaussian, Inc.: Wallingford, CT, 2004.
- (56) Finkelmeier, H.; Lüttke, W. *J. Am. Chem. Soc.* **1978**, *100*, 6261.
- (57) Kamińska-Trela, K.; Bernatowicz, P.; Lüttke, W.; Machinek, R.; Trættemberg, M. *Magn. Reson. Chem.* **2002**, *40*, 640.

CT7003287